Chapter 10

Passive Data Association Techniques for Unambiguous Location of Targets

This chapter was written, in part, by Henry Heidary of Hughes Aircraft Corporation (*now Raytheon Systems*)*, Fullerton, CA.*

Sensor and data fusion can occur using several types of passively acquired information. For example, the raw signals themselves or various types of information extracted from the signals may be selected as inputs to data fusion processors. The signals, sensor data, and communications media available in a particular command-and-control system often dictate the optimum data fusion technique. This chapter addresses data fusion architectures applicable to multiple sensor and multiple target scenarios in which range information to the target is missing, but where the target location is required.

10.1 Data fusion options

Unambiguous target track files may be generated by using data association techniques to combine various types of passively acquired data from multiple sensors. In the examples described in this chapter, multiple ground-based radars are used to locate energy emitters, i.e., targets, by fusing either of three different types of received data: (1) received signal waveforms, (2) angle information expressing the direction to the emitters, or (3) emitter angle track data that are output from the sensors. The alternate fusion methods illustrate the difficulties and system design issues that arise in selecting the data fusion process and the type of passively acquired data to be fused.

These fusion techniques allow range information to be obtained from arrays of passive sensors that measure direction angles, or from active sensors where range information is denied (as for example when the sensor is jammed), or from combinations of passive and active sensors. For example, electronic support measure (ESM) radars can use the fused data to find the range to the emitters of interest. These fusion methods can also be used with surveillance radars that are jammed to locate the jammer positions. In a third application, angle data from a netted array of IRST sensors, or for that matter from acoustic or any passively operated sensors, can be fused to find the range to the emitters.

Fusion of the signal waveforms received from the emitters or the direction angles to the emitters is supported by a centralized fusion architecture. Fusion of the emitter angle track data is implemented with a decentralized architecture.

As shown in Figure 10.1, the first centralized fusion architecture combines the signal waveforms received at the antenna of a scanning surveillance radar, acting in a receive-only mode, with those from another passive receiver. The second passive receiver searches the same volume as the surveillance radar with a nonscanning, high-directivity multibeam antenna. The detection data obtained from the scanning and nonscanning sensors are used to calculate the unambiguous range to the emitters. This fusion approach allows the positions of the emitters to be updated at the same rate as data are obtained from the surveillance radar, making timely generation of the surveillance volume and emitter target location possible. One coherent processor is required for each beam in the multibeam antenna. A large communications bandwidth is also needed to transmit the radar signals to the multibeam passive receiver. The passive receiver is collocated with the coherent processors where the data fusion operations are performed.

In the second centralized fusion example, bearing angle-only data that describe the direction to the emitters are measured by multiple surveillance radars operating in a receive-only mode. The angle measurements are sent to a centralized location where they are associated to determine the unambiguous range to the emitters. Either elevation and azimuth angles or only azimuth angle

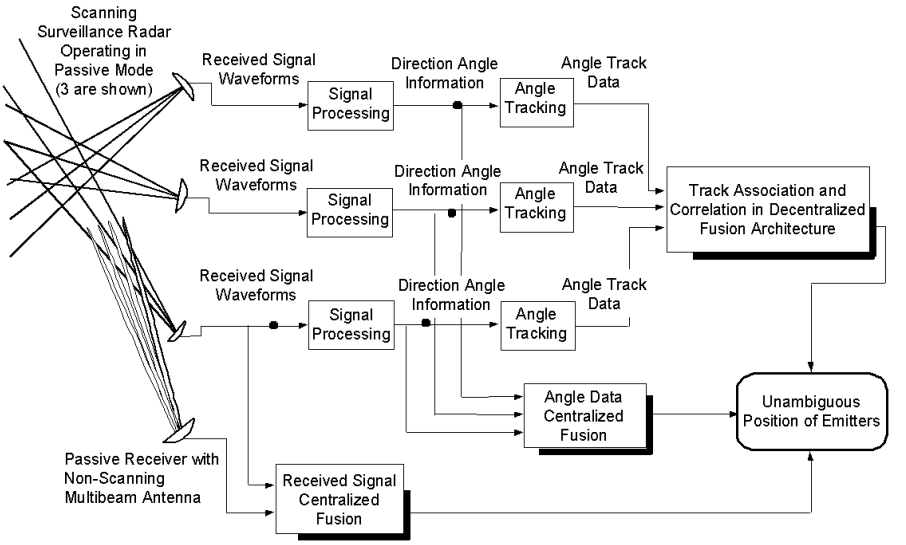

Figure 10.1 Passive sensor data association and fusion techniques for estimating location of emitters.

measurements can be used as the input data to this fusion process. Ghost intersections, formed by intersecting radar beams for which targets do not exist, are eliminated by searching over all possible combinations of sensor-angle data and by selecting the most likely angle combinations for the target positions. The large number of searches needed to find the optimal direction angle-target associations may require high processor throughput, which is a controlling factor in determining the feasibility of this fusion architecture when large numbers of emitters are present. The data association process is modeled using a maximum likelihood function. Two methods are discussed to solve the maximum likelihood problem. In the first method, the maximum likelihood process is transformed into its equivalent zero-one integer-programming problem to find the optimal associations. In the second method, the computational requirements are reduced by applying a relaxation algorithm to solve the maximum likelihood problem. Although the relaxation algorithm produces somewhat suboptimal direction angle-emitter associations, in many cases they are within approximately 1 percent of the optimal associations.

The decentralized fusion architecture combines the multiscan tracks produced by the individual surveillance radars. The time history of the tracks, which contain the direction angles to the airborne emitters, aids in the calculation of the unambiguous range and eliminates the need for the large numbers of searches required when deghosting is necessary. If angle tracks from only one passive sensor are available, it is still possible to estimate the range to the emitter if the tracking sensor is able to perform a maneuver. This latter case requires a six state Kalman filter as explained toward the end of the chapter.

All these techniques allow the unambiguous location of the emitters to be calculated. However, the impact on processing loads, communication bandwidths required for data transmission, and real-time performance differs. Advantages and disadvantages of each approach for processing passively acquired data are shown in Table 10.1, where a linkage is also made to the fusion architectures described in Chapter 3. Each of the techniques requires system-level trades as discussed in the appropriate sections below.

10.2 Received-signal fusion

The first centralized fusion architecture called received-signal fusion, combines the signal waveforms received by a scanning surveillance radar with those from a nonscanning (in this example) passive receiver that incorporates a multibeam antenna to search the volume of interest. The signals from these two sensors are transmitted to a central processor, where they are coherently processed to produce information used to locate the source of the signals.

The advantages of this architecture include unambiguous location of the emitter targets without creating ghosts that are characteristic of the angle data fusion

architecture.[1] Ghosts occur when we believe there is a target present, but in truth there is no target present. Received-signal fusion requires transmission of large quantities of relatively high-frequency signal data to a centralized processor and, therefore, received-signal fusion places a large bandwidth requirement on the communications channel.

Table 10.1 Fusion techniques for associating passively acquired data to locate and track multiple targets.

Fusion Level	Data Fusion Technique	Advantages	Disadvantages
• Received Signal (pixel-level fusion)	Coherent processing of data received from two types of sensors: a scanning surveillance radar and a passive receiver with a high-directivity multibeam antenna	• All available sensor information used • Unambiguous target location obtained • Data are processed in real time	• Large bandwidth communications channel required • Auxiliary sensor required • One coherent processor for each beam in the multibeam antenna required
• Angle Data (feature-level fusion)	Maximum likelihood or relaxation algorithm using direction angle measurements to the target	• 3D position of target obtained • Communication channel bandwidth reduced	• Ghosts created that have to be removed through increased data processing
• Target Track (decision-level or sensor-level fusion)	Combining of distributed target tracks obtained from each surveillance radar	• 3D position of target obtained • Communication channel bandwidth reduced even further	• Many tracks must be created, stored, and compared to eliminate false tracks

In the coherent processing technique illustrated in Figure 10.2, the scanning surveillance radar signals are combined with those from a multibeam antenna to compute the time delay and Doppler shift between the surveillance radar and multibeam antenna signals. These data, along with the instantaneous pointing direction of the surveillance radar, allow the position and velocity of the emitters to be estimated using triangulation techniques, for example.

The multibeam receive-only antenna is assumed to contain a sufficient number of beams to search the surveillance region of interest. The emitters indicated with "plus" symbols in Figure 10.2 represent this region. The coherent processors operate jointly on the surveillance radar signal and the multibeam antenna signals

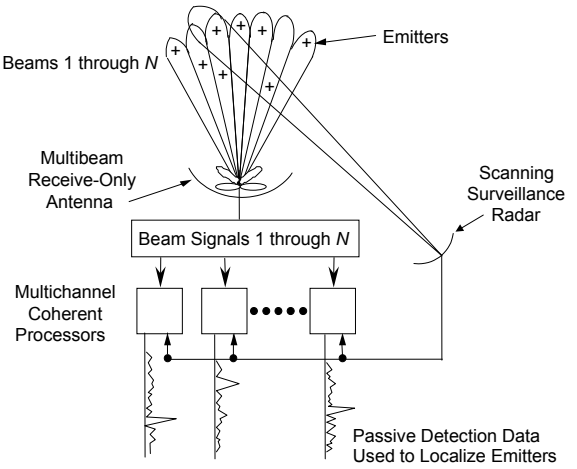

Figure 10.2 Coherent processing of passive signals.

to simultaneously check for the presence of emitters in all the regions formed by the intersecting beams. The ambiguity of declaring or not declaring the presence of an emitter in the observation space is minimized by the coherent processing. The multibeam antenna and the bank of coherent processors permit emitter positions to be calculated faster than is possible with angle data fusion. In fact, the emitter location information is available in real time, just as though the surveillance radar was making the range measurement by itself. In addition, coherent processing allows for simultaneous operation of the surveillance radar as an active sensor to detect targets in a nonjammed environment and also as a passive receiver to locate the emitters in a jammed environment.

10.2.1 Coherent processing technique

Knapp and Carter[2] and Bendat and Piersol[3] have suggested a method to reliably infer if one of the signals received by the multibeam antenna and the signal received by the surveillance radar emanate from a common source and are independent of a signal coming from another emitter. Their method treats the multibeam antenna and radar signals as random processes and calculates the dependence of the signal pairs using a cross-correlation statistic that is normalized by the energy contained in the two signals.

For our application, the Knapp and Carter cross-correlation statistic $\gamma(t)$ is given by

$$\gamma(t)=\frac{\left|\int_{t-T}^{t} x(t)\,y(t-\tau)\exp(-2\pi j\,\mathrm{v}\,t)dt\right|}{\left[\int_{t-T}^{t}\left|x(t)\right|^2 dt\int_{t-T}^{t}\left|y(t-\tau)\right|^2 dt\right]^2}, \tag{10-1}$$

where $x(t)$ and $y(t)$ represent the complex value of the two random processes (signals) over the immediate prior time interval T, which is equal to the signal processing time. The variables τ and ν are estimates of the relative time delay and Doppler shift frequency, respectively, between the signals received by the multibeam antenna and surveillance radar from the common emitter source.

The $\gamma(t)$ statistic is particularly effective when the noise components in the signal are uncorrelated. In this case, Knapp and Carter show that the performance of a hypothesis test (deciding if an emitter is present or not) based on the cross-correlation statistic depends on (1) the signal-to-noise ratio (SNR) calculated from the power received at the multibeam antenna and the surveillance radar and (2) the time-bandwidth product formed by the product of the signal processing time T and the limiting bandwidth of the system. The limiting bandwidth is the smallest of the multibeam antenna receiver bandwidth, surveillance radar bandwidth, coherent processor bandwidth, or the communications channel bandwidth. In high-density emitter environments with relatively low SNRs, the cross-correlation statistic provides a high probability of correctly deciding if a signal is present for a given, but low value of the probability of falsely deciding that an emitter is present.

A typical result of the Knapp and Carter statistic for wideband coherent signals is shown in Figure 10.3. On the left are the real and imaginary parts of the signal received by the multibeam antenna. On the right are the corresponding signals received by the surveillance radar. The waveform at the bottom represents the output of the coherent processor. Estimates of the Doppler shift ν are plotted against estimates of the time delay τ. If the received signals come from the same emitter, then for some value of ν and τ there will be a large-amplitude sharp peak in the value of γ. If the peak is above a predetermined threshold, an emitter is declared present. The emitter's location is computed from the law of sines applied to the triangle formed by the baseline distance between the surveillance radar and the multibeam antenna, and the azimuth direction angles to the emitter as measured by the surveillance radar and multibeam antenna. The trigonometry for the calculation is shown in Figure 10.4. Since the radar is rotating, the relative time delay τ gives a correction for the azimuth direction angle of the radar in the law of sines range calculation. The elevation of the emitter is also known from the sensor data.

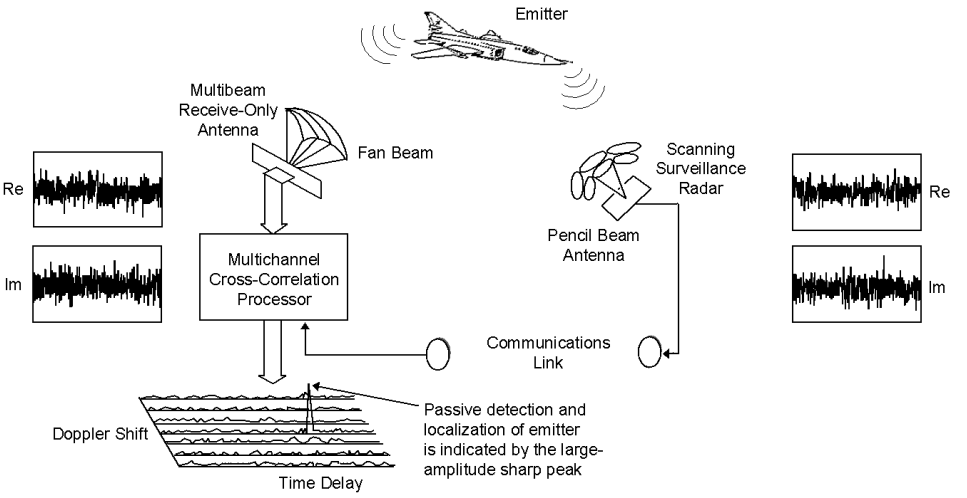

Figure 10.3 Cross-correlation processing of the received passive signals.

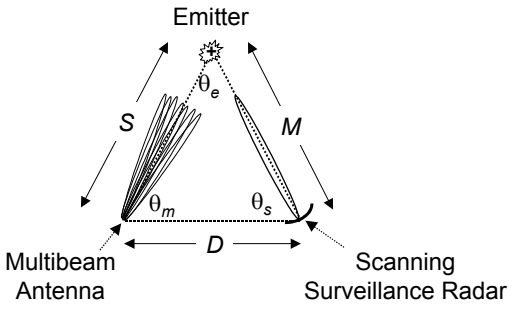

From law of sines:

- $D/\sin\theta_e = M/\sin\theta_m = S/\sin\theta_s$
- D, θ_m, θ_s are known from measurements
- $\theta_e = 180 - \theta_m - \theta_s$
- Distance S from multibeam antenna to emitter is $S = D \sin\theta_s/\sin\theta_e$
- Distance M from surveillance radar to emitter is $M = D \sin\theta_m/\sin\theta_e$

Figure 10.4 Law of sines calculation of emitter location.

10.2.2 System design issues

The major subsystems in the received-signal fusion architecture are the surveillance radar, the multibeam antenna including its beamforming network, the communication link between the surveillance radar and the coherent processors, and the coherent processors themselves. Table 10.2 lists the key issues that influence the design of the coherent-receiver fusion architecture.

The system's complexity and performance are determined by the relationships between the design parameters. Complexity is affected by the throughput requirements for the coherent processor, the design of the passive multibeam antenna, and the bandwidth and jam resistance of the surveillance radar-to-processor communication channel. Throughput requirements for the coherent processor depend on the number of beams, the number of time-delay and

Doppler-shift cells that must be searched for a maximum in the cross-correlation signal, and the processing gain required for the hypothesis test that determines whether the signals emanate from a common source. The number of beams is dependent on the resolution of the multibeam antenna and its angular field of view. Processing gain depends on SNR, which in turn depends on the spatial and amplitude distributions of the emitters in relation to the angular resolution of the radar and multibeam antenna.

Table 10.2 Major issues influencing the design of the coherent receiver fusion architecture.

Issue	Design Impact
• Spatial and amplitude distribution of emitters	• Angular resolution • Baseline separation • Processing gain
• Emitter velocity	• Number of Doppler cells
• Coherence of transmission media as it affects emitter signals	• Processing gain
• Angular resolution of surveillance radar and multibeam antenna	• Number of time-delay cells • Signal-to-noise ratio
• Baseline separation between surveillance radar and multibeam antenna	• Communications requirements (amplifiers, repeaters, noise figure, etc.) • Number of time-delay cells
• Processing gain	• Throughput of coherent processors
• Simultaneous operation of radar and multibeam antenna	• Signal-to-noise ratio
• Directivity of radar and multibeam antenna	• Number of coherent processors • Sensitivity of multibeam antenna receiver
• Resistance to jamming of baseline communications channel	• Communications techniques (spread spectrum, time-division multiple access [TDMA], etc.)

The range of time delays that must be searched in the coherent processor depends directly on the angular resolutions of the radar and multibeam antenna.[4] The number of time-delay cells is proportional to the total amount of delay normalized by the signal observation interval T. The upper bound of the observation interval is given by the radar angular resolution divided by its angular search rate.

The range of Doppler shift that must be searched to locate emitters depends on the angular field of view of the system.[4] The number of Doppler-shift cells in the coherent processor is proportional to the total amount of Doppler shift normalized by the signal bandwidth. For broadband emitters, the upper bound to the signal bandwidth is given by the bandwidth of the radar transfer function. Within the constraints imposed by the radar, it is feasible to independently choose various values for observation interval and signal bandwidth, such that their product equals the required time-bandwidth product for the coherent processing. The computations associated with the coherent processing are minimized when the observation interval and signal bandwidth are optimized through trades among observation interval, number of time-delay cells, bandwidth, and number of Doppler-shift cells.

Surface and volume clutter will adversely affect the SNR at both the surveillance radar and multibeam antenna. The quantitative effects depend on the effective radiated power and directivity of the radar, the directivity of the multibeam antenna, and the amplitude distribution characteristics of the clutter in the radar's field of view. Coherent processor performance is affected by the amplitude and phase components of the signal at the input to the coherent processor. The signal bandwidth, in turn, depends on the transmission medium's temporal and spatial coherence statistics, the nonlinearities of the radar and multibeam antenna response functions, and the amplitude and phase transfer functions of the baseline communications channel.

The distance between the radar and multibeam antenna affects the performance of the fusion system in four significant ways: (1) radar-to-multibeam antenna communication requirements including jammer resistance and signal amplification and filtering, (2) range of time delays that must be searched by the coherent processor, (3) mutual surveillance volume given by the intersection of the radar and multibeam antenna fields of view, and (4) accuracy with which the emitters are located. Typical separation distances between the radar and multibeam antenna are 50 to 100 nautical miles (93 to 185 km). In addition, the topography along the radar-to-multibeam antenna baseline influences the applicability of a ground-to-ground microwave communications link.

10.3 Angle data fusion

In the second centralized fusion architecture, referred to as angle data fusion, multiple surveillance radars (operating in a receive-only mode) are utilized to measure the elevation and azimuth angles that describe the direction to the emitters. These data are fused in a central processor to find the number of real emitters and estimate the unambiguous range to each. Associating multisensor data at a given time instant, as required in this fusion architecture, is analogous to associating data from the successive scans of a single sensor to form tracks.[5]

The major design elements of the passive surveillance radar system are the antenna, the detection and data association processes, and the communication link between the radars and the central processing unit. IRST sensors can also passively track these targets. When they are used, sensor separation can be reduced to between 10 and 15 nautical miles (19 to 28 km) because of the IRST's superior angle measurement accuracy as compared to microwave radars.

10.3.1 Solution space for emitter locations

If there are M radar receivers and N emitters in the field of view of the radars, then associated with each emitter is an M-tuple of radar direction angle measurements that uniquely determines the position of the emitter. When the number of direction angle measurements made by each radar is equal to N, there are as many as N^M unique direction M-tuples, or potential emitter locations, to sort through since the true position of the emitters is unknown.

Not all M-tuple combinations represent real locations for the emitters. For example, there are M-tuples that will place multiple emitters at the same direction angle and thereby invalidate the number of independent measurements known to be made by a particular radar. This is illustrated in Figure 10.5.

Three emitter locations are known to have been detected by the radar on the left as represented by the three direction angle measurements emanating from M_1. Two emitter locations are known to have been detected by the radar on the right as represented by the two direction angle measurements emanating from M_2. The detection of only two emitters by the radar on the right can occur when two of the three emitters lie on the same direction angle or the radar's resolution is inadequate to resolve the emitters. In Figure 10.5, Emitters 1 and 2 are placed on the left-most direction angle and Emitter 3 on the middle direction angle measured by Radar 1, leaving no emitters on the right-most direction angle. This combination represents a fallacious solution that must be excluded since the premise of three direction angle measurements by Radar 1 is not represented. The false positions are eliminated by constraining the solution to contain the

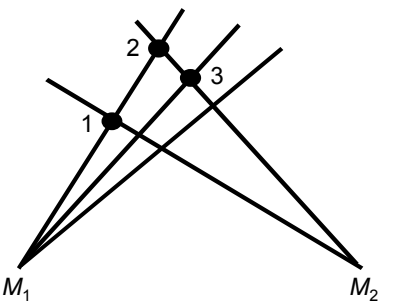

Figure 10.5 Unacceptable emitter locations.

same number of emitter direction angle measurements as corresponds to the radar data and to use each angle measurement only once. Since there are N emitters, there are only N true positions to be identified. Thus there are $N^M - N$ ambiguous M-tuple locations to be eliminated, because these represent locations for which there are no emitters.

When the number of direction angle measurements from each of the radars is not equal, the number of potential locations for the emitters must be found in another manner. The procedure for this case is illustrated by the example in Figure 10.6.

Six potential locations for three emitters jamming two radar receivers are illustrated. However, only one set of intersections formed by the direction angle measurements corresponds to the real location of the emitters. The upper part of the figure shows that the first radar measures angle data from all three emitters as indicated by the three lines whose direction angles originate at point M_1. The number of angle measurements is denoted by $N_1 = 3$. The second radar, due to its poorer resolution or the alignment of the emitters or both, measures angle data from only two emitters as shown by the two direction angles that originate at point M_2. Here the number of angle measurements is denoted by $N_2 = 2$. The total number of intersections is equal to $N_1 \times N_2 = 6$. The six potential solutions that result are illustrated in the lower portion of the figure. The problem is to

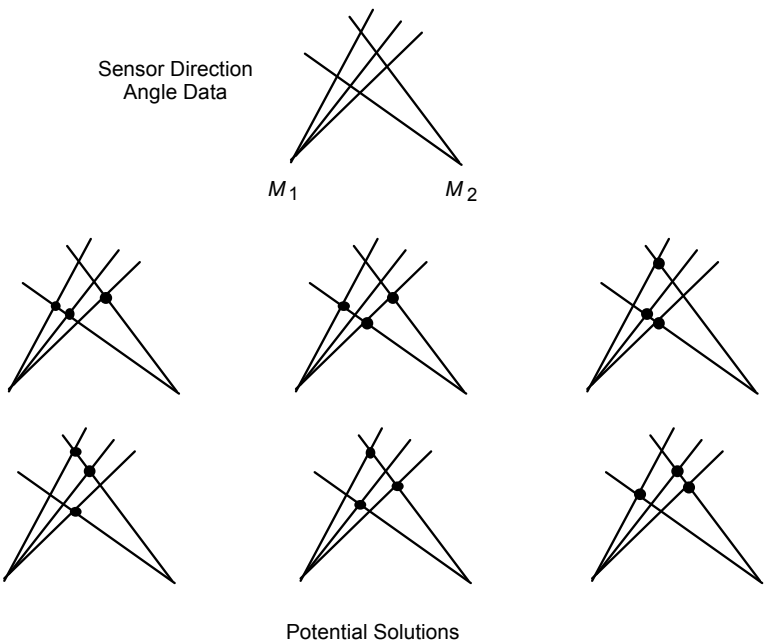

Figure 10.6 Ambiguities in passive localization of three emitter sources with two receivers.

identify the solution that gives the best estimate for the location of the three emitters.

Figure 10.7 illustrates the ambiguities that arise for a generalization to N emitters and three radars. The upper portion of the figure shows the number of angle measurements made by each radar, namely, N_1, N_2, and N_3. The lower left shows the intersection of the three radar beams with the N emitters. The total number of intersections is given by $N_1 \times N_2 \times N_3$.

The graph in the lower right of the figure contains four curves. The upper curve, labeled "All Possible Subsets," represents the N^M unique solutions that correspond to the direction angle measurements made by each of the three radars. The curve labeled "Possible Subsets with Constraints" represents the number of unique solutions assuming that an angle measurement is used only once to locate an emitter. The bottom two curves result from simulations that use prefiltering without and with an efficient search algorithm, respectively, to remove unlikely intersections. The prefilter examines the intersection space formed by the radar direction angle measurements and eliminates those having intersection areas greater than some preset value. Intersections located behind any of the radars are

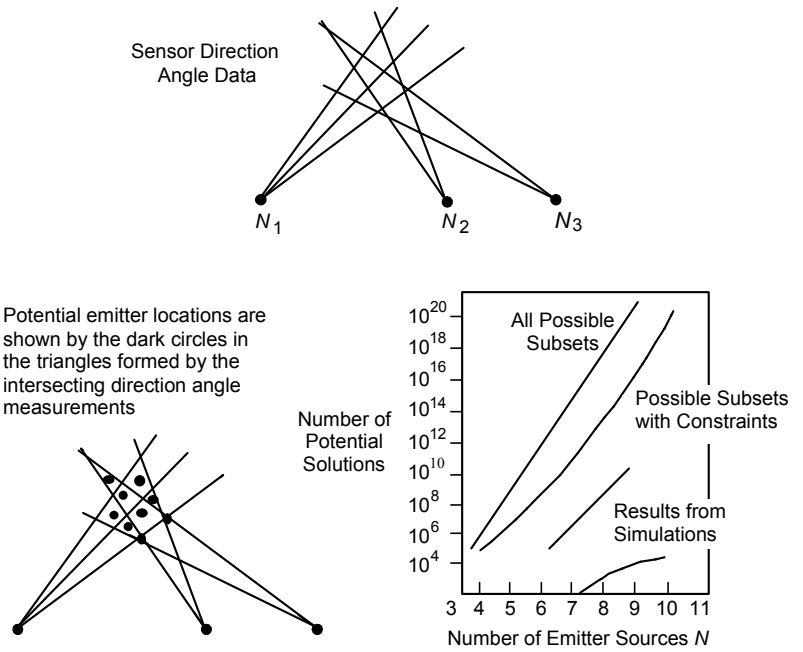

Figure 10.7 Ambiguities in passive localization of N emitter sources with three receivers.

also eliminated. Clearly the prefiltering reduces the number of potential solutions. Using an efficient search algorithm with the prefilter (efficient in terms of the number of iterations required to reach an optimal or near optimal solution), such as the set partitioning and relaxation algorithms discussed in the next section, reduces the number of potential solutions even further as shown in the bottom curve. However, the number of potential solutions remains large (of the order of 10^4), even for the modest numbers of emitter sources shown.

If the radars measure both azimuth and elevation-angle data, the search algorithm is simplified considerably. In this case, a two-dimensional assignment algorithm can be used and the requirement for a three-radar system is reduced to a two-radar system.

The numbers of densely positioned emitter sources and radar resolution determine algorithm performance and throughput. In these environments, algorithms must (1) make consistent assignments of radar angle measurements to emitter positions while minimizing ghost and missed emitter positions, (2) fuse direction angle information from three or more radars that possibly have poor resolution in an environment where multipath may exist, and (3) be efficient for real-time or near real-time applications in their search of the number of potential solutions and the assigning of *M*-tuples to emitters.

The first data association technique discussed for the three-radar system uses zero-one integer programming to find the optimal solution by efficiently conducting a maximum likelihood search among the potential *M*-tuples. The azimuth direction measurements obtained from the radars are assigned to the *N* emitter locations with the constraint that each angle measurement be used only once in determining the locations of the emitters. Prefiltering is employed to reduce the direction angle-emitter association (*M*-tuple) space.

The second technique uses a relaxation algorithm to speed the data association process that leads to the formation of *M*-tuples. The relaxation algorithm produces suboptimal solutions, although simulations have shown these angle measurement associations to be within 1 percent of the optimal.

10.3.2 Zero-one integer programming algorithm development

Consider a planar region where *N* emitters or targets are described by their Cartesian position (*x, y*). Assume that the targets lie in the surveillance region of the radars and are detected by three noncollocated radar sensors (having known positions and alignment) that measure only the azimuth angle Θ from the emitter relative to north. The statistical errors associated with each radar's directional measurement are assumed to be Gaussian distributed with zero mean and known variances. In addition, spurious directional measurement data, produced by phenomena such as multipath, are present and are uniformly distributed over the

field of view of each sensor. We call an emitter location estimable if all three radars detect the direction angle (in this case the azimuth angle) to the emitter. We shall calculate the positions for only the estimable emitters, but not for those that are unresolved by the radars.

The solution involves partitioning the angle measurements into two sets, one consisting of solutions corresponding to the estimable emitter positions and the second corresponding to spurious measurements. Spurious data are produced by multipath from azimuth angle measurements and the N^3 minus N 3-tuples that represent ambiguous positions generated by the incorrect association of azimuth angles.

Partitioning by the maximum likelihood function selects the highest probability locations for the emitters. The maximum likelihood function L is the joint probability density function corresponding to the emitter locations. It is given by[6]

$$L = \prod_{\gamma \in \Gamma} \frac{1}{(2\pi)^{3/2}} |\Sigma|^{-1/2} [\exp(-1/2\,\Theta_b^T\, \Sigma^{-1}\, \Theta_\gamma)](1/\Phi_1)^{m_1 - N}\,(1/\Phi_2)^{m_2 - N}\,(1/\Phi_3)^{m_3 - N} \tag{10-2}$$

where

Γ = set of all possible 3-tuples that represents the real and ambiguous emitter locations,

γ = 3-tuple of radar angle data that is believed to correspond to a particular emitter,

Σ = diag $[\sigma_1^2, \sigma_2^2, \sigma_3^2]$,

σ_r^2 = variance of the angle measurements associated with the r^{th} radar (r = 1, 2, and 3 in this example),

Φ_r = field of view of the r^{th} radar, $0 \le \Phi_r \le 2\pi$,

m_r = number of direction measurements associated with Radar r for one revolution of the radar,

N = number of emitters,

Θ_γ = particular 3-tuple vector of direction angle measurements from Radars 1, 2, and 3,

= $[\Theta_{1i}, \Theta_{2j}, \Theta_{3k}]^{\mathrm{T}}$ where i, j, and k refer to a particular direction angle measurement from Radars 1, 2, and 3, respectively, and

T = transpose operation.

To facilitate the search over all possible 3-tuples, the maximum likelihood problem is replaced with its equivalent zero-one integer-programming problem. The zero represents nonassignment of direction angle measurements to a 3-tuple, while the one represents assignment of direction angle measurements to a 3-tuple, with one direction angle being assigned from each radar.

Maximization of the likelihood function is equivalent to minimizing a cost function given by the negative of the natural logarithm of the likelihood function shown in Eq. (10-2). The use of the cost function and a set of constraints allows the original problem to be solved using the zero-one integer programming algorithm.

When the fields of view of the three radars are equal such that $\Phi_1 = \Phi_2 = \Phi_3 = \Phi$, the cost function C can be written in the form

$$C = (m_1 + m_2 + m_3)\ln\Phi + \sum_{i=1}^{m_1}\sum_{j=1}^{m_2}\sum_{k=1}^{m_3}(C_{ijk} - 3\ln\Phi)\delta_{ijk} \tag{10-3}$$

where

$$C_{ijk} = \Theta_\gamma^{\mathrm{T}}\, \Sigma^{-1}\, \Theta_\gamma \tag{10-4}$$

subject to

$$\sum_i \sum_j \delta_{ijk} \le 1 \text{ for all } k, \tag{10-5}$$

$$\sum_i \sum_k \partial_{ijk} \le 1 \text{ for all } j, \tag{10-6}$$

and

$$\sum_j \sum_k \delta_{ijk} \le 1 \text{ for all } i, \tag{10-7}$$

where

$$\delta_{ijk} = 1 \tag{10-8a}$$

when the i^{th} direction angle from Radar 1, the j^{th} from Radar 2, and the k^{th} from Radar 3 are selected, and

$$\delta_{ijk} = 0 \tag{10-8b}$$

when these direction angles are not selected.

The constraint is to use an angle measurement from a radar only once in forming the 3-tuples. This constraint may cause an emitter location to be missed when the radar resolution is not adequate to provide one measurement for each emitter, or when the emitters are aligned such that some are blocked from the view of the radars. These drawbacks will, over time, resolve themselves due to emitter motion and the geometry of the search situation.

Throughput requirements can be reduced by eliminating solutions that make the term (C_{ijk} – 3 lnΦ) positive, such as by preassigning $\delta_{ijk} = 0$ for these solutions, because this always decreases the value of the cost function. With the above constraint and the elimination of positive cost function solutions, the zero-one integer programming problem is converted into the standard set-packing problem formulation,[7] solved by using any set-partitioning algorithm such as those described by Pierce and Lasky[8] and Garfinkel and Nemhauser.[9] Further simplification is made by eliminating still other variables, such as those representing small costs, even though they are negative. This produces a suboptimal 3-tuple, but considerably reduces the number of searches required to solve the zero-one integer programming problem. Since three radars are used in this example, the integer programming is solved with a three-dimensional assignment algorithm as described by Frieze and Yadegar.[10]

Figures 10.8 through 10.10 show the results of applying the above techniques to a scenario containing 10 emitters and 3 radars. The emitters, referred to as the "True Targets," were randomly placed along a racetrack configuration as shown by the dark squares in Figure 10.8. The racetrack was approximately 60 nautical miles (111 km) north of the radars located in (x, y) coordinates at (-50, 0), (0, 0), and (50, 0) nautical miles (50 nautical miles equals 93 km) as depicted by the "star" symbols along the x-axis. Radar resolution was modeled as 2 degrees. The standard deviation of the radar angle measurements was assumed to be 0.5 degree.

Figure 10.9 shows all the possible subsets of candidate target positions, represented by open circles before prefiltering and the other constraints were applied. In Figure 10.10, prefiltering reduces the number of possible target positions processed by the zero-one integer-programming algorithm. The final result of applying the cost constraints and the zero-one integer programming is shown in Figure 10.8 by the open circles. Positions of 8 of the 10 true emitter targets were correctly identified. The two targets that were not located lie within 2 degrees of each other and, therefore, could not be detected with the radar resolution limit of 2 degrees used in this example. Since the targets are moving, however, this system would be able to resolve all the emitter targets as their separation increased with time to beyond 2 degrees.

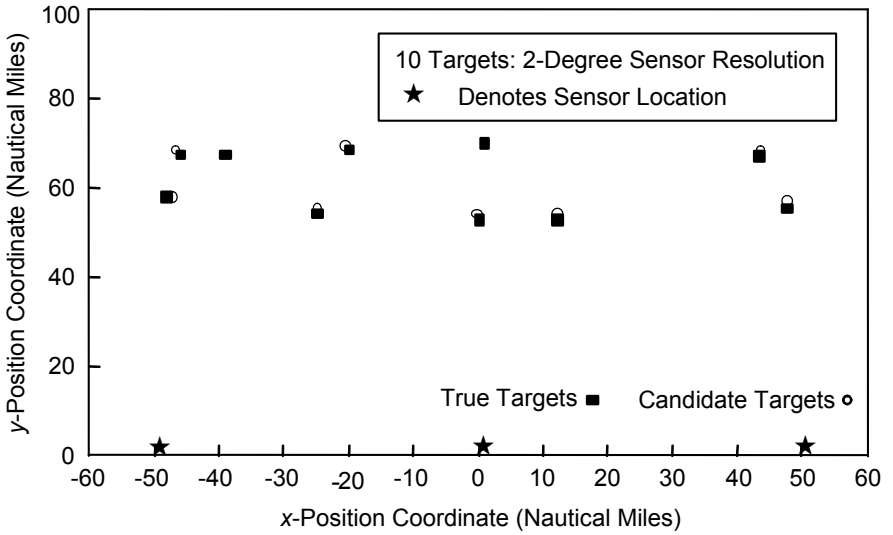

Figure 10.8 Passive localization of 10 emitters using zero-one integer programming.

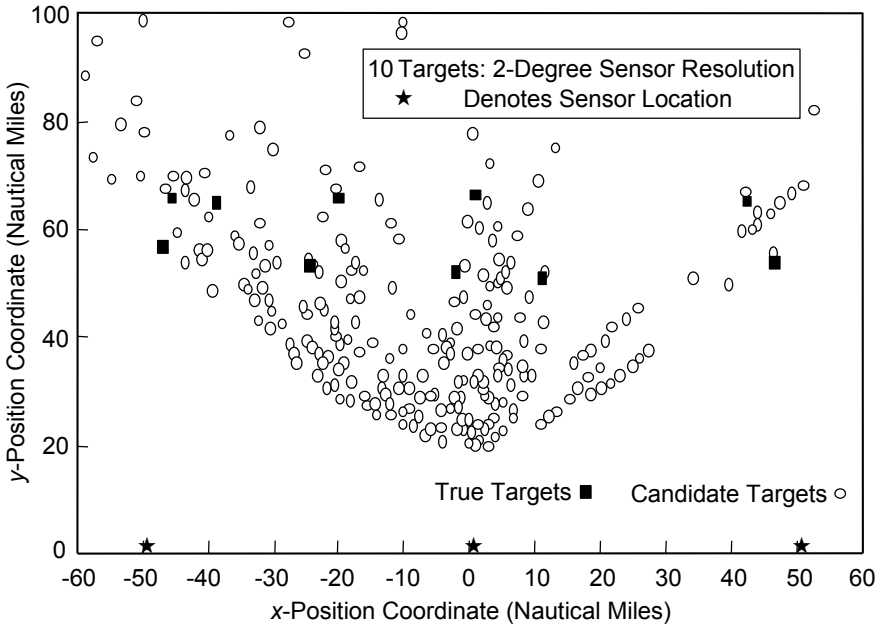

Figure 10.9 All subsets of possible emitter positions before prefiltering and cost constraints are applied.

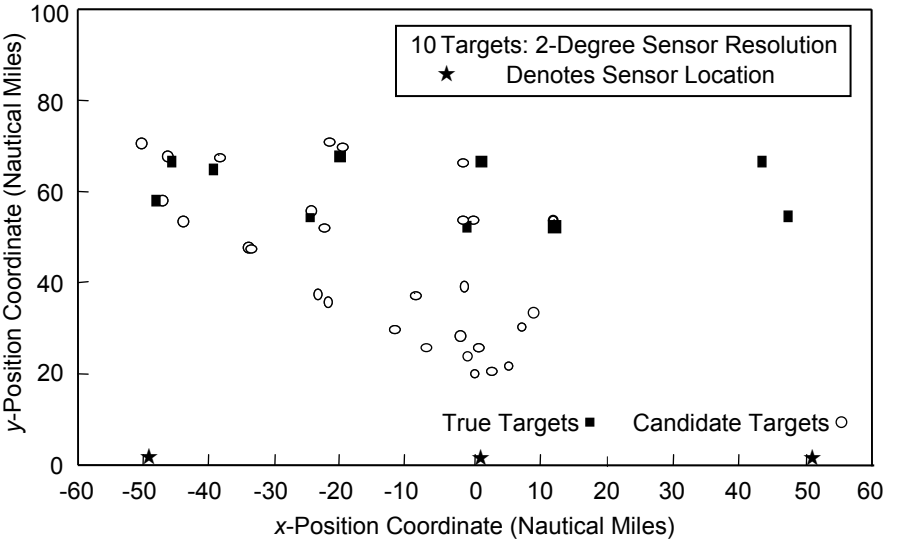

Figure 10.10 Potential emitter positions that remain after prefiltering input to zero-one integer programming algorithm.

High-speed computers reduce the computation time required by the zero-one integer programming approach. A calculation with a Macintosh IIsi incorporating a Motorola 68030 20-MHz processor and coprocessor provided solutions to the 10-target problem using 2 to 3 seconds of central processor unit (CPU) time per radar scan.[11] Another host using a Sky Computers Skybolt VME board containing one i860 processor (80 MFLOPS) reduced the CPU time to less than 0.2 second with 10 targets and less than 1.3 seconds with 20 targets.

These CPU usage times are per run averages based on 10 runs. State-of-the-art, faster executing microprocessors are expected to reduce the CPU time by a factor of 10 to 100. Since long-range surveillance radars have scan rates of about 10 seconds, it is feasible to implement these algorithms in near real time with a restricted number of targets. However, as the number of potential targets increases, real-time execution of the zero-one integer programming technique becomes more difficult. This is due to the exponential increase in the complexity of the optimal algorithm with the number of measurements made by each sensor, since the algorithm has nonpolynomial computational time and memory requirements. Suboptimal algorithms such as the relaxation algorithm are, therefore, of considerable importance, as they require smaller computational times.

10.3.3 Relaxation algorithm development

The search time through potential solutions can be decreased using a Lagrangian relaxation algorithm.[12] With this approach, near optimal solutions (producing

sensor data association *M*-tuples within approximately 1 percent of the optimal) can be obtained for reasonable computing times with moderate numbers of emitters (of the order of 20). In the development by Pattipati et al., unconstrained Lagrange multipliers are used to reduce the dimensionality of the three-dimensional data assignment problem to a series of two-dimensional assignment problems. A heuristic strategy that recomputes the data association at every iteration of the solution minimizes the cost of the suboptimal solution as compared with the optimal. A desirable feature of this method is the estimate it produces of the error between the feasible suboptimal solution and the global optimal solution. The error may be used to control the number of iterations.

Algorithm run time is a function of the sparsity of the search volume and the number of reports from each sensor. Sparsity is defined as the ratio of the average number of potential direction angle measurement-emitter associations in the three-dimensional assignment problem to the number of angle measurement-emitter associations required for a fully connected graph. The graph represents the *M*-tuple associations of the sensor measurements with emitters. For example, if a graph has 10 nodes (where a node is the number of reports per sensor), there are $10^3 = 1000$ angle measurement-emitter associations with a three-sensor system. If there are *M* angle measurement-emitter associations instead, the sparsity of the graph *S* is

$$S = \frac{M}{1000}. \tag{10-9}$$

Therefore, a larger value of *S* implies a greater graph density.

Data in Table 10.3 (from Pattipati, et al.) show the speedup provided by the relaxation algorithm over a branch-and-bound algorithm[13] averaged over 20 runs. (The algorithm described by Pierce and Lasky[8] also provides improved results over the branch-and-bound, but not as much as the relaxation algorithm.)

Branch-and-bound algorithms perform a structured search for a solution. They are based on enumerating only a small number of the possible solutions because the remaining solutions are eliminated through the application of bounds. The branch-and-bound algorithm involves two operations: branching, i.e., dividing possible solutions into subsets, and bounding, i.e., eliminating those subsets that are known not to contain solutions. The basic branch-and-bound technique is a recursive application of these two operations.[14,15]

The branch-and-bound algorithm was found impractical for graphs containing 500 or more angle measurement-emitter associations. Hence, the speedup was not computed for these cases. The average run time of the relaxation algorithm on a Sun 386i is shown in parentheses. For these particular examples, the average solution to the angle measurement-emitter association problem was within 3.4

percent of optimal. As the sparsity decreases, the percent of suboptimality also decreases. In another example cited by Pattipati, the worst case suboptimal solution was within 1.2 percent of the optimal when the sparsity was 0.25 and the number of reports per sensor was 10.

Table 10.3 Speedup of relaxation algorithm over a branch-and-bound algorithm (averaged over 20 runs). (K.R. Pattipati et al., *IEEE Trans. Auto. Cont.*, 37(2), 198-213 [Feb. 1992].)

Number of Reports From Each Sensor	Sparsity = 0.05	Sparsity = 0.1	Sparsity = 0.25	Sparsity = 0.5	Sparsity = 1.0
5	1.2 (0.006)*	1.6 (0.01)	1.7 (0.04)	2.2 (0.2)	16.6 (0.4)
10	3.0 (0.02)	3.8 (0.06)	30.3 (0.6)	3844.0 (1.4)	† (2.3)
15	4.8 (0.16)	26.4 (0.27)	1030.4 (2.1)	† (3.6)	† (5.8)
20	18.5 (0.2)	656.1 (0.44)	† (2.3)	† (7.5)	† (12.1)

* The numbers in parentheses denote the average time, in seconds, required by the relaxation algorithm on a Sun 386i workstation.

† Denotes that memory and computational resources required by the branch-and-bound algorithm exceeded the capacity of the Sun 386i (5 MIPS, 0.64 MFLOPS, 12 Mb RAM) workstation.

Although the relaxation algorithm provides fast execution, there is no guarantee that an optimal or near optimal solution with respect to cost gives the correct association of angle measurements to emitters. In fact, as the sensor resolution deteriorates, it becomes more difficult to distinguish the true emitters from ghosts.

10.4 Decentralized fusion architecture

The decentralized fusion architecture finds the range to the emitters from the direction angle tracks computed by receive-only sensors located at multiple sites. These tracks are formed from the autonomous passive azimuth and elevation angle data acquired at each site. The tracks established by all the sensors are transmitted to a fusion center where they are associated using a metric. Examples of metrics that have been applied are the distance of closest approach of the angle tracks and the hinge angle between a reference plane and the plane formed by the emitters and the sensors.[16] The range information is calculated from trigonometric relations that incorporate the measured direction angles and the known distances between the sensors.

A number of Kalman filter implementations may be applied to estimate the angle tracks. In the first approach, each sensor contains a multistate Kalman filter to track azimuth angles and another to track elevation angles. The number of states is dependent on the dynamics of the emitter. In another approach, the azimuth and elevation angle processing are combined in one filter, although the filters and fusion algorithms are generally more complicated. In either implementation, the azimuth and elevation angle Kalman filters provide linearity between the predicted states and the measurement space because the input data (viz., azimuth and elevation angles) represent one of the states that is desired and present in the output data.

Data analysis begins at each sensor site by initiating the tracks and then performing a sufficient number of subsequent associations of new angle measurement data with the tracks to establish track confidence. The confidence is obtained through scan-to-scan association techniques such as requiring n associations out of m scans. An optimal association algorithm, such as an auction algorithm, can be used to pair emitters[17] seen on scan n to emitters observed on the following scan $n + 1$. The set of emitters on scan $n + 1$ that are potential matches are those within the maximum relative distance an emitter is expected to move during the time between the scans. A utility function is calculated from the distance between the emitters on the two scans. The auction algorithm globally maximizes the utility function by assigning optimal emitter pairings on each scan.

The performance of the auction algorithm is shown in Figure 10.11. The average association error decreases as the sensor resolution increases and the interscan time decreases. The angle tracks produced at an individual sensor site are not sufficient by themselves to determine the localized position of the emitters. It is necessary to transmit the local angle track files to the fusion center, where redundant tracks are combined and the range to the emitters is computed and stored in a global track file.

10.4.1 Local optimization of direction angle track association

The simplest decentralized architecture fuses emitter tracks by first estimating the time histories of the angle tracks produced by each sensor and then pairing them using a metric that measures the distance between the tracks. Tracks are associated when the metric is less than a preselected threshold. This technique does not globally optimize the track association among the sensors because the track pairings are not stored or recomputed after all tracks and data have been analyzed. Local track optimization was used in early air defense systems to track the objects detected by the sensors.

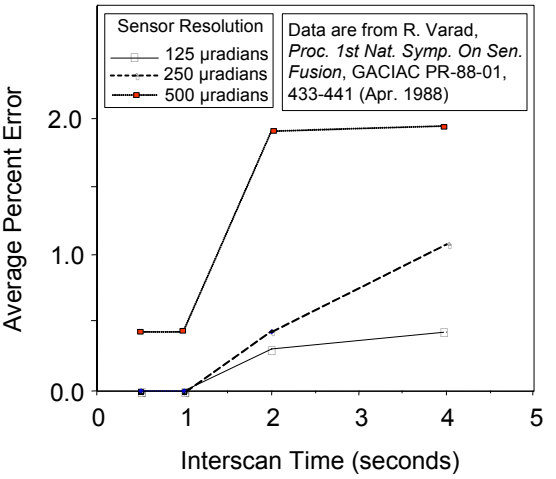

Figure 10.11 Average scan-to-scan association error of auction algorithm over 15 scans. (S.E. Kolitz, *Proc. SPIE* 1481, 329-340 [1991].)

To locally optimize track association, the first track produced by Sensor 1 is selected and compared with the first track produced by Sensor 2. A metric such as the chi-squared (χ^2) value of the distance at the point of closest approach of the direction angle tracks (which is equal to the Mahalanobis distance) is calculated for each pairing. If the value exceeds a threshold, the pairing is discarded since the threshold exceedance indicates that the particular pairing will not produce the desired probability that the two tracks are from the same emitter. The track from Sensor 1 is then compared with the next track from Sensor 2. The process continues until the χ^2 value is less than the threshold. At this point, the angle tracks are combined, as they are believed to represent the same emitter. *Paired tracks from Sensors 1 and 2 are removed from the lists of available tracks and the next track from Sensor 1 is selected for association with a track from Sensor 2 that is still unpaired.*

The process continues until all tracks from Sensor 1 are associated or until the list is exhausted. Unpaired tracks are retained for later association with the unpaired tracks from the other sensors. If a third set of angle tracks is available from a third sensor, they are associated with the fused tracks from the first two sensors by repeating the above process. Again unpaired tracks are retained. After all the sets of available angle tracks have been through the association process, the unpaired tracks from one sensor are compared with unpaired tracks from sensors other than the one used in its initial parings. If the χ^2 value of the distance at the point of closest approach of the tracks is less than the threshold, the tracks are paired and removed from the unpaired list. Unpaired tracks arise because one sensor may not detect the target during the time another sensor measured a track. The technique just described is analogous to a first-in, first-out approach with respect to the selection of pairings for the tracks from Sensor 1.

10.4.2 Global optimization of direction angle track association

Two methods of globally optimizing the association of the direction angles measured by the sensors will be discussed. The first applies a metric based on the closest approach distance of the direction angle tracks. The second uses the hinge angle. Global optimization is achieved at the cost of some increased computational load as compared with the local optimization method.

Closest approach distance metric

To globally optimize the track association with the closest approach distance metric, a more complex algorithm is needed such as the Munkres algorithm,[18] its extension by Bourgeois and Lassalle,[19] or the faster executing JVC[20] algorithm. The advantage of these algorithms comes from postponing the decision to associate tracks from the various sensors until all possible pairings are evaluated. In this way track pairings are globally optimized over all possible combinations. The process starts as before by selecting the first track from Sensor 1 and comparing it with the first track from Sensor 2. If the χ^2 value for the closest approach distance of the track direction angles exceeds the threshold, the pairing is discarded and the track from Sensor 1 is compared with the next track from Sensor 2. The process continues until χ^2 is less than the threshold. At this point, the angle tracks are combined as they are believed to represent the same emitter and the value of χ^2 is entered into a table of track pairings. However, the paired track from Sensor 2 is not removed from the list as before. *Also, the process of pairing the first track from Sensor 1 with those of Sensor 2 continues until all the tracks available from Sensor 2 are exhausted.* Whenever χ^2 is less than the threshold value, the χ^2 value corresponding to the pairing is entered into the table of pairings. This approach can therefore identify more than one set of potential track pairings for each track from Sensor 1.

Then the next track from Sensor 1 is selected for association and compared with the tracks from Sensor 2 beginning with the first track from the Sensor 2 track list. *Tracks from Sensor 2 used previously are made available to be used again in this algorithm.* If the χ^2 value exceeds the threshold, the pairing is discarded, and the track from Sensor 1 is compared with succeeding tracks from Sensor 2. When the χ^2 value is less than the threshold, that value is entered into the table of track pairings.

The process continues until all tracks from Sensor 1 are associated or until the lists are exhausted. Unpaired tracks are retained for later association with the unpaired tracks from the other sensors. If a third set of angle tracks is available from a third sensor, they are associated with the fused tracks from the first two sensors by repeating the above process.

Global optimization of the track pairings occurs by using the Munkres or the faster executing JVC algorithm to examine the χ^2 values in the table that have been produced from all the possible pairings. Up to now, the χ^2 value only guarantees a probability of correct track association if the angle tracks are used more than once. The Munkres and JVC algorithms reallocate the pairings in a manner that minimizes the sum of the χ^2 values over all the sensor angle tracks and, in this process, the algorithms use each sensor's angle tracks only once.

The acceptance threshold for the value of χ^2 is related to the number of degrees of freedom n_f, which, in turn, is equal to the sum of the number of angle track measurements that are paired in the Sensor 1 tracks and the Sensor 2 tracks. Given the desired probability for correct track association, the χ^2 threshold corresponding to n_f is determined from a table of χ^2 values.

Hinge angle metric

The hinge angle metric allows immediate association of detections to determine the emitter position and the initiation of track files on successive scans. Calculations are reduced, as compared to the Munkres algorithm, by using a relatively simple geometrical relationship between the emitters and the sensors that permits association of detections by one sensor with detections by another. The metric allows ordered sequences of emitters to be established at each sensor, where the sequences possess a one-to-one correspondence for association.

Processing of information from as few as two sensors permits computation of the hinge angle and the range to the emitters. However, each sensor is required to have an attitude reference system that can be periodically updated by a star tracker or by the Global Positioning System, for example. It is also assumed that the sensors have adequate resolution to resolve the emitters and to view them simultaneously. Occasionally, multiple emitters may lie in one plane and may not be resolvable by all the sensors. However, the emitters will probably be resolved during subsequent scans. The use of three sensors mitigates this problem.

The hinge angle procedure defines a unique emitter target plane based on the line-of-sight (LOS) vector from a sensor to a particular emitter and the line joining the two sensors as shown in Figure 10.12. Each emitter target plane contains the common LOS vector between the two sensors and each can be generated by a nominal reference plane rotated about the LOS vector between the two sensors. The angle between the emitter target plane and the reference plane is

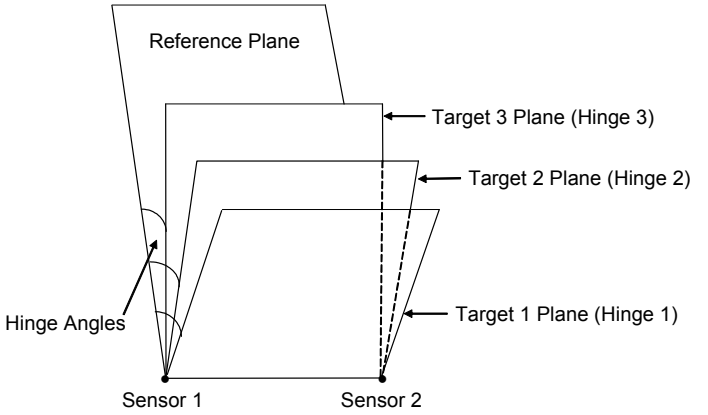

Figure 10.12 Varad hinge angle.

called the hinge angle. The reference plane is defined by Varad[16] to contain the unit normal to the LOS vector between the sensors. Kolitz[17] defines the reference plane to contain the origin of the inertial coordinate system and extends Varad's procedure for utilizing data from three sensors.

Hinge angle association reduces the computational burden to a simple single parameter sort. The sorting parameter is the angle between the nominal reference plane and the plane containing the sensor and emitter target. The sets of scalar numbers, i.e., the direction cosines representing the degree of rotation of the reference plane into the sensor-emitter plane, are ordered into monotonic sequences, one sequence for each sensor. Ideally, in the absence of noise and when all sensors view all emitters, the sequences of the angles representing the emitters will be identical. Thus, there is a one-to-one correspondence between the two ordered sequences, resulting in association of the emitters. In the nonideal real-world application, the Varad algorithm matches up each emitter in the sequence of planes produced by one sensor, with an emitter having the closest hinge angle in the sequence produced by another sensor.

Once the hinge angles from the two sensors are associated, the range to the emitter is computed from the known angles between the LOS vectors to the emitter and the LOS vector between the sensors. Since the distance between the sensors is known, a triangle is defined with the emitter located at the third apex. The range can be calculated using the law of sines as discussed in conjunction with Figure 10.4.

10.5 Passive computation of range using tracks from a single sensor site

Range to the target can also be estimated with track data from a single passive sensor that performs an appropriate maneuver.[21,22] In two dimensions, a Kalman filter using modified polar coordinates (MPC) is suitable for tracking non-

maneuvering targets. These coordinates reduce problems associated with observability, range bias, and covariance ill conditioning that are encountered with Cartesian coordinates. The MPC filter is extended to three dimensions by converting to modified spherical coordinates (MSC). The states in the Kalman tracking filter now include two angles, two angle rates, inverse time to go (equal to range rate divided by range), and inverse range. These states are transformable into Cartesian position and velocity.

The MSC filter can be applied to find the range to targets that are either nonmaneuvering or maneuvering. If the target does not maneuver, the range state decouples from the other states in the tracking filter. If the target is maneuvering, then a batch estimation method (one that processes all of the observations simultaneously) is used to predict the future state of the target. Thus, maneuver detection must be an integral part of any successful range estimation algorithm in order to properly interpret the data from a single tracking sensor. A conventional approach to maneuver detection compares a chi-squared statistic based on the difference between the actual and expected measurement (also called the residual) with a threshold. If the chi-squared statistic is excessive (e.g., exceeds a confidence level of approximately 0.999), then a maneuver is declared present. A return to a nonmaneuver state occurs when the chi-squared statistic falls below a lower threshold. Other statistics are used to detect slow residual error accumulations.

10.6 Summary

Three data fusion techniques have been introduced for locating targets that emit energy. They are used with passive tracking systems or when it is anticipated that data otherwise available from active systems, including range information, will be unattainable. These techniques associate the data using either central or decentralized fusion architectures, with each having its own particular impact on data transmission and processing requirements.

In the first centralized fusion architecture, signals passively received by a surveillance radar and signals received through an auxiliary multibeam antenna are coherently processed. The resulting cross-correlation function expresses the likelihood that the signals received by the surveillance radar and multibeam antenna originated from the same source. This technique has a large impact on communications facilities because large-bandwidth raw signals need to be transmitted over potentially large distances. The impact on signal processing is equally large because of the range of time delays and Doppler shift that must be processed to include large search areas.

The second centralized fusion architecture combines azimuth direction angles or azimuth and elevation direction angles that are computed by each radar receiver. The major concern here is the elimination of ghost signals caused by noise or

poor search geometry. Because processed data are transmitted to the central fusion processor, the communications channel bandwidth requirements are reduced as compared to those from the first architecture. The use of a maximum likelihood function allows the computation of an optimal solution for data association. The angle measurements are partitioned into two sets, one consisting of solutions corresponding to estimable emitter target positions and the other to spurious measurements. The final location of the emitter targets is found by converting the maximum likelihood formulation of the problem into a zero-one integer-programming problem that is more easily solved. Here a zero is assigned to direction angle information from a radar that does not maximize the location of an emitter, and a one is assigned to information that does. The zero-one integer-programming problem can be efficiently solved by applying constraints, such as using each radar's angle measurement data only once and eliminating variables that do not contribute to the maximization of the likelihood function. A suboptimal solution that significantly speeds up the data association process can also be found. This solution, which uses a relaxation algorithm, is particularly valuable when the number of emitters is large.

In the decentralized fusion architecture, still more processing is performed by individual radars located at distributed sites. High-confidence angle tracks of the emitter targets are formed at each site from the locally acquired sensor data using scan-to-scan target association or an auction algorithm. The tracks, along with unassociated data, are transmitted to a fusion center, where they are associated with the tracks and data sent from other sites. Two sensor-to-sensor track association methods were discussed: (1) a simple technique that eliminates sensor tracks already paired from further association, and (2) two global optimization techniques that allow all tracks from one sensor to be associated with all tracks from other sensors. The chi-squared value of the distance of closest approach of the tracks or the hinge angle is used to globally maximize the correct association of tracks and data received from the multiple sensor sites. Since most of the emitter location data have been reduced to tracks, the communications bandwidth required to transmit information to the fusion center is reduced even further. However, greater processing capability is required of the individual sensors.

An approach that allows range to be computed using angle tracks estimated by a single sensor was also discussed. This technique requires the tracking sensor to engage in a maneuver and to ascertain whether the tracked object has maneuvered or not.

References

1. D.E.N. Davies, "High data rate radars incorporating array signal processing and thinned arrays," *International Radar Conference Record*, Pub. 75CHO938-1 AES, IEEE, Piscataway, NJ (Apr. 1975).
2. C.H. Knapp and C.C. Carter, "The generalized correlation method for estimation of time delay," *IEEE Trans. Acoust., Speech, Signal Processing*, A(4), 320-327 (Aug. 1976).
3. J.S. Bendat and A.G. Piersol, *Engineering Applications of Correlation and Spectral Analysis*, John Wiley and Sons, New York, NY (1980).
4. H. Heidary, Personal communication.
5. Y. Bar-Shalom and T.E. Fortmann, *Tracking and Data Association*, Academic Press, New York, NY (1988).
6. P.R. Williams, "Multiple target estimation using multiple bearing-only sensors," *Proceedings of the 9th MIT/ONR Workshop on C3 Systems*, Report LIDS-R-1624, Massachusetts Institute of Technology, Laboratory for Information and Decision Systems, Cambridge, MA (December 1986).
7. E. Balas and M. Padberg, "Set partitioning: a survey," *SIAM Rev.*, 18, 710-760 (Oct. 1976).
8. J.F. Pierce and J.S. Lasky, "Improved combinatorial programming algorithms for a class of all zero-one integer programming problems," *Management Sci.*, 19, 528-543 (Jan. 1973).
9. R. Garfinkel and G. Nemhauser, *Integer Programming,* John Wiley and Sons, New York, NY (1972).
10. A.M. Frieze and J. Yadegar, "An algorithm for solving three-dimensional assignment problems with application to scheduling a teaching practice," *J. Op. Res. Soc.*, 32(11), 989-995 (1981).
11. P.R. Williams, personal communication.
12. K.R. Pattipati, S. Deb, Y. Bar-Shalom, and R.B. Washburn, Jr., "A new relaxation algorithm and passive sensor data association," *IEEE Trans. Automat. Control*, 37, 198-213 (Feb. 1992).
13. D.B. Reid, "An algorithm for tracking multiple targets," *IEEE Trans. Automat. Control*, AC-24, 423-432 (Dec. 1979).
14. E. Lawler and E. Wood, "Branch-and-bound methods: A survey," *J. Op. Res.*, 14, 699-719 (1966).
15. R. Babuska, *Fuzzy Modeling for Control*, Kluwer Academic Publishers, Boston, MA (1998).
16. R. Varad, "Scalar correlation algorithm: Multi-target, multiple-sensor data fusion," *Proc. of the 1st National Symposium on Sensor Fusion*, GACIAC PR-88-01, 433-441 (Apr. 1988).
17. S.E. Kolitz, "Passive sensor data fusion," *Signal and Data Processing of Small Targets*, *Proc. SPIE* 1481, 329-340 (1991).
18. J. Munkres, "Algorithms for the assignment and transportation problem," *J. SIAM*, 5, 32-38 (Mar. 1957).

19. F. Bourgeois and J.C. Lassalle, "An extension of the Munkres algorithm for the assignment problem to rectangular matrices," *Comm. Association for Computing Machinery*, 802-804 (1971).
20. O.E. Drummond, D.A. Castanon, and M.S. Bellovin, "Comparison of 2-D assignment algorithms for sparse, rectangular, floating point, and cost matrices," *J. SDI Panels Tracking,* Institute for Defense Analyses, Alexandria, VA, Issue No. 4/1990, 4-81 to 4-97 (Dec. 15, 1990).
21. D.V. Stallard, "Angle-only tracking filter in modified spherical coordinates," *J. Guidance*, 14(3), 694-696 (May-June 1991).
22. R.R. Allen and S.S. Blackman, "Implementation of an angle-only tracking filter," *Signal and Data Processing of Small Targets*, *Proc. SPIE* 1481, 292-303 (1991).